LUNDS UNIVERSITET

Development of chemical kinetic mechanisms for combustion of hydrocarbons with fluorinated compounds

Frej Ryde

Thesis submitted for the degree of Master of Science
Project duration: 4 months

Supervised by Elna Heimdal Nilsson

Department of Physics
Division of Combustion Physics
May 2021

Abstract

Electric vehicles are becoming more common as one of many solutions to the increasingly serious problem of global warming. This comes with new safety challenges as batteries can upon malfunction or abuse enter thermal runaway and as a result catch fire or explode. The gases released from thermal runaway has been determined experimentally in published studies and have been shown to contain fluorinated compounds. Fluorinated compounds have not been thoroughly studied in the larger context of combustion chemistry and there are therefore no standard chemical kinetic mechanisms with fluorinated compounds in them. The goal of this project is to create a chemical kinetic mechanism that can use fluorinated compounds and other, in the combustion research, less common hydrocarbons, such as dimethyl carbonate. The chemical kinetic mechanism was then used in simulations of ignition delay time and flame propagation speed. It was found that mixing fluorinated compounds with other hydrocarbons had a small effect on the ignition time and flame speed. It was also found that a mixture of two compounds will have a flame speed and ignition time between the flame speed and ignition time of mixtures composed of the pure compounds.

Contents

1 Introduction **4**

2 Background **6**

2.1 Battery fires 6

2.2 Literature review 7

2.2.1 Measurement methods 7

2.2.2 Composition of vented gases 8

2.2.3 Composition of combustion products 9

2.3 Combustion simulations 9

2.4 Chemical kinetics 11

3 Methods **14**

3.1 Simulations 14

3.2 Mechanisms 14

3.3 Mixtures 15

4 Results **17**

4.1 Ignition times 17

4.2 Flame speed 20

5 Discussion **23**

5.1 Ignition time 23

5.2 Flame speed 25

6 Outlook **27**

7 Acknowledgments **28**

8 Appendix **30**

List of abbreviations and acronyms

BMS	Battery management system
DEC	Diethyl carbonate
DMC	Dimethyl carbonate
EV	Electronic vehicle
EA	Ethyl acetate
EMC	Ethyl methyl carbonate
EC	Ethylene carbonate
FID	Flame ionization detector
FTIR	Fourier transform infrared spectroscopy
GC	Gas chromatography
LLNL	Lawrence Livermore national laboratories
LIB	Lithium–ion battery
LCO	Lithium–cobalt–oxide cathode
LFP	Lithium–iron–phosphate cathode
LMO	Lithium–manganese–oxide cathode
NMC	Lithium–nickel–manganese–cobalt–oxide cathode
LTO	Lithium–titanium–oxide cathode
MS	Mass spectroscopy
NDIR	Non-dispersive infrared analysis
PC	Propylene carbonate
TCD	Thermal conductivity detector
DMC–mech	Mechanism developed by Alexandrino et al. 2018 [23]
F–mech	Mechanism developed by Linteris et al. 2020 [24]
DMC+F–mech	Combined mechanism

List of Symbols

r	Reaction rate
S	Concentration of specie S
t	Time
k	Rate constant
c_i	Constant for the i:th species
T	Temperature
E_A	Activation energy
R	Ideal gas constant
A	Reaction specific constant
n	Reaction specific constant
s	Stochiometric coefficient

1 Introduction

The average temperature of the earth is currently increasing due to human activities. One of the activities that contributes to this problem of global warming is the transportation of goods and people in human society. Most vehicles used for transportation rely on an internal combustion engine. Fossil fuels are burnt in the engines and gases, such as carbon dioxide, are released into the air where they are a health hazard or contribute to global warming. One method to combat this problem is to avoid using vehicles with an internal combustion engine, and instead use electrical vehicles powered by electricity from renewable sources. This is probably one of the reasons why electric vehicles are becoming more popular as the problems with global warming are becoming more apparent and severe. The sales of electric vehicles have increased significantly during the last decade [1], as seen in Figure 1.

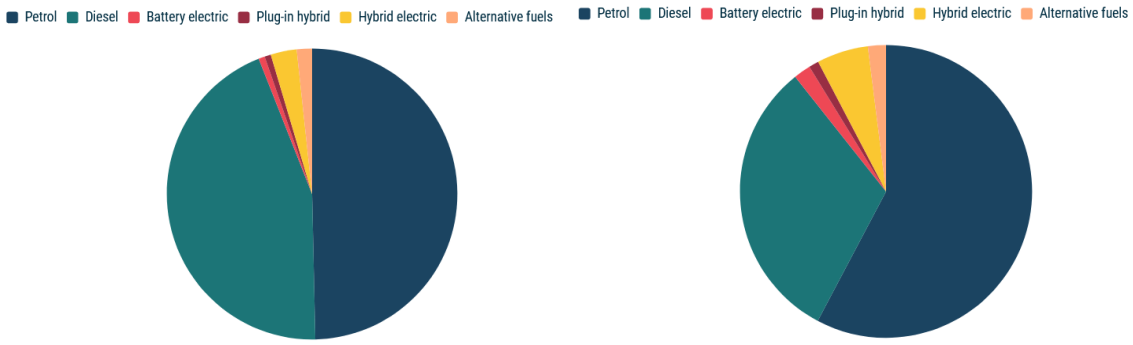

Figure 1: Sales of new passenger cars based on fuel type from 2017 (left) and 2019 (right) [1]

While electric vehicles is a way to avoid the negative consequences of the internal combustion engine, they present new technical challenges and safety concerns. The electric energy must be stored inside a battery and the currently most common battery is the lithium-ion battery. Lithium-ion batteries have a high energy density compared to other types of batteries and are cheap enough to be produced in sufficient amounts to use in a large number of electric vehicles. They are also safe to use and handle during normal operation. However, if a lithium-ion battery is abused or it malfunctions, there is a risk that it will enter a state called thermal runaway. In this state, a chain of exothermic reactions occur that increase the temperature of the battery. The increase in the temperature of the battery increases the rate of the reaction, which further increases the temperature. As such, one gets a uncontrollable increase of the temperature in the battery, called a thermal runaway. The reactions do not only produce heat, but also different gases that build up during the thermal runaway and with the build up of gases, the pressure inside the battery cell increases. The thermal runaway results in the venting of the gases via a preassigned venting route, or the battery may break or explode, releasing all of the gases into the surrounding. The released gases can catch fire once exposed to the outside air. An example of this can be seen in Figure 2 where an electric car has caught fire after an accident. A battery fire or explosion can cause sever damages on people or property in the vicinity. Furthermore some of the gases that are released from the battery or produced in the fire are toxic.

Some of the gases released from batteries in thermal runaway are well known from regular combustion, like small hydrocarbons, carbon monoxide and carbon dioxide. Other gases are less common in regular combustion systems, but are of large importance in battery fires. One type of compounds that are released from the battery contains fluoride. They are called fluorinated compounds and they are of a special interest as they are often toxic. Hydrofloric acid is an example of a compound containing fluoride that can be released from a battery after a fire or thermal runaway. Hydrofluoric acid is not a commonly known compound for the lay audience, but the chloride counterpart, hydrochloric acid, is more well know. Hydrofluoric acid is less acidic than hydrochloric acid, but it is very poisonous and one does not need to drink or inhale much to pass a lethal dose. As such, there is a large interest in preventing hydrofluoric acid from being released from the battery directly or as a product gas in the battery fire [2].

Figure 2: An electric car that has caught fire after an accident [3]

Thermal runaway and accidents with batteries happen very seldom, but when they do happen, it is a disaster and the accidents need to be prevented. However, the current understanding of the gases released and the following combustion process is lacking, and research is needed in both areas before the batteries can be improved. The knowledge required to improve the batteries could be obtained both from physical experiments and from computer simulations.

The problem with simulations of fire including fluorinated compounds is that they are currently not included in standard computer simulation packages of combustion. Kinetic mechanisms are needed to make a computer simulation of a combustion process and the kinetic mechanisms currently lack fluorinated compounds. This is very problematic as computer simulations could be a powerful tool in the understanding of battery fires and the design of safe battery systems. All properties of a combustion process are not easy to measure. The temperature of the combustion can readily be measured experimentally, but the concentration of the species in the combustion is difficult to measure. However, computer simulation of combustion gives these concentrations easily. Furthermore, it is simple to make small adjustments to the objects that are simulated, while a physical experiment might require that the objects are remade from scratch. Physical objects also need to be remade between experiments as the combustion consumes the object. As such, computer simulations are good at testing a large number of cases and can therefore be used in screening to find the relative small number of interesting cases. Then these cases can be experimentally tested.

The purpose of the project reported here is to develop and use a kinetic mechanism including fluorinated compounds in combination with hydrocarbons of relevance to battery fires. A kinetic mechanism is a collection of all the species, reactions and rates of the reactions that take part of the combustion. The kinetic mechanism will be used to study the ignition time and flame propagation resulting from gas mixtures that could be released from a battery after thermal runaway. To do this, the current understanding of what is released from a battery that has entered thermal runaway or caught fire has been found by studying the scientific literature in this subject. Then an already existing reaction mechanism for relevant hydrocarbons was found from the literature and modified to include also fluoride compounds and reactions containing the fluoride compounds.

2 Background

2.1 Battery fires

Most vehicles are relatively heavy machines that are supposed to travel fast. As such, any power source needs to contain a lot of energy. A typical battery in an electric vehicle (EV) must produce a power of hundreds of kW to accelerate the vehicle and have a capacity of tens of kWh to give a long driving range [4]. At the same time, other practical restrictions are placed on the batteries as they should be small to fit into the EV, have a low weight to not add to the mass of the EV more than necessary and cheap to be viable as an economic alternative. These restrictions are quite harsh and the current solution is to pack multiple battery cells together into modules and modules are arranged together into a battery pack [5]. The cells have to be protected from external factors that could damage them and the packs need to be held together when exposed to vibrations. This means that each battery pack needs internal structure for protection, but this causes a problem. The temperature inside a battery pack is difficult to manage, even though most battery packs have a battery management system (BMS) installed [7]. The BMS is constructed to manage the power output, charging, discharging and temperature. Cooling loops are used to regulate the temperature, state-of-charge monitoring to regulate charging and discharging, and cell-charge balancing to regulate the power of the battery [6].

The difficulty of temperature management is further exacerbated if the battery cells enter thermal runaway. A battery cell can enter thermal runaway if it is abused or if it malfunctions. Examples of abuse includes mechanical damage, overheating and overcharge. The problem with the battery will trigger a group of chemical reactions. The reactions are, overall, exothermal and will therefore increase the temperature of the battery. This causes the rate of the reactions to increase, which further increases the temperature. This feedback loop between the temperature and the rate of the reactions will continue until all of the gases are vented or the battery breaks. As the chemical reactions produce gases, this often happens when a safety control in the form of a vent is triggered that releases the gases from the battery. If the vent fails to trigger, the gases inside the battery will build up a large pressure until the battery mechanically explodes. The gases released from the battery after the thermal runaway have a high temperature and they might spontaneously ignite or they may ignite by other ways.

An exploding battery that catches fire is a major concern that could severely injure anyone nearby and cause sever damage to surrounding property. The fact that the battery might be in an EV traveling along a highway in high speeds further increases the danger. Moreover, a potential fire or explosion is not the only associated danger with thermal runaway. If the gases are properly vented and do not explode, they may be inhaled by nearby humans or animals. Measurements of the composition of the gases released from batteries that has entered thermal runaway or burned will be discussed more in the next section, but some of them are highly toxic. Two examples of such gases are carbon monoxide and hydrogen fluoride. Carbon monoxide is well known from incomplete combustion and is not only toxic, but also hard to detect by people. Breathing in air containing 3% carbon monoxide can lead to death [8].

As stated earlier, the most popular battery type in EVs is the lithium-ion battery (LIB). However, there are multiple variants of LIB:s. Three common variants that will appear in this report are the LFP, NMC and LCO cells. The difference between these cell types is the other materials that accompany the lithium-ions in the cathode. The LFP cells have a lithium–iron–phosphate cathode, NMC cells have a $Li(Ni_xMn_yCo_z)O_2$ cathode and the LCO cells have a $LiCoO_2$ cathode [12]. The NMC cells have different amounts of the metals, but the sum of x, y and z is usually one. Blended NMC and LCO cells also exist and will be called NMC/LCO cells. Two less common battery types are the lithium magnesium oxide, LMO, and the lithium titanate oxide, LTO. The exact composition of a cell varies as outlined above and these variations in the composition results in differences in the thermal runaway processes and in the composition of the released gases. The batteries also have different compositions of the electrolytes, which will be discussed later in this thesis. Batteries also differ in other aspects like the physical housing and relative size of the components. Golubkov et al. 2014 measured the composition of three types of cells, LFP, NMC and NMC/LCO [12]. Different parts of the

batteries varied in size and mass. For example, the batteries were between 17 and 27% housing, 7 and 17% anode and 25 and 41% cathode. The electrolyte was between 10 and 16% of the total mass of the battery. This is of interest as the electrolyte takes part in the reactions that drives the thermal runaway and some of the electrolyte follows the gases out of the battery. Fernandes et al. 2018 used only the LFP type of battery, but they measured the composition of the electrolyte [11]. The main components of the electrolyte in that study were dimethyl carbonate, DMC, ethyl methyl carbonate, EMC, propylene carbonate, PC, and ethylene carbonate, EC.

2.2 Literature review

Several studies have measured the gases released from a battery that have undergone thermal runaway. A summary of the results from key studies is presented in Table 1. The table also presents what method was used to detect released gases and, in some cases, how much of each gas was released. This is important as all methods are not able to detect all species and some methods require the user to look for a certain species.

The literature review presented in this section is an essential part of the present work since it acts as a foundation to select relevant gas mixtures to investigate using simulations. Previous experimental studies have measured both vent gases escaping the battery after thermal runaway, and product gases from the resulting fire. Both aspects are reviewed. The studies are summarized in Tables 1 and 2.

2.2.1 Measurement methods

The most common method to detect species is Fourier-transform infrared spectroscopy, FTIR, used by Sturk et al. 2018 [9], Fernandes et al 2018 [11] and all studies presented in Table 2. This is an optical method using the absorption of infrared light to detect species. It is different from most other forms of spectroscopy in that many different wavelengths of light are used at different intensities and the absorption data is then analysed by using a Fourier-transformation.

Another optical method is the non-dispersive infrared analysis, NDIR, which was used by Truchot et al. 2018 [15] and Lecocq et al. 2016 [16]. It compares the absorption of infrared light, IR, from a source in the analyser that has passed through either a chamber with a known gas or a chamber with the sample gas. The non-dispersive part comes from the fact that the analyser does not use dispersive optical elements, like a prism or a diffraction grating, to select specific wavelengths to measure.

A third method used to detect gases is the flame ionization detector, FID, which was used by Sturk et al. 2018 [9], Truchot et al. 2018 [15] and Lecocq et al. 2016 [16]. It employs the fact that ions are produced when a hydrocarbon is undergoing combustion. A hydrogen flame is used to combust the gas sample and thereby to create the ions and an electrode pair is used to separate the ions from the rest of the flame. This method can not detect which hydrocarbons are in the sample, but it can detect the mass of the hydrocarbons.

Another method that uses ions is mass spectrometry, MS, used by Sturk et al. 2018 [9]. The sample is ionized and the ions are then led into a homogeneous magnetic field. The ions will then diverge from a straight path based on the mass and charge of the ion, which is used to identify the ion.

Gas chromatography, GC, is a method to separate species from each other and is used in combination with other methods by Sturk et al. 2019 [9], Golubkov et al. 2014 [12] and Yuan et al. 2020 [13]. The sample is lead through a tube together with a carrier gas. The gases in the sample will take different amounts of time to pass through the tube based on how the gas interacts with the carrier gas compared to the inner wall of the tube. GC is used to separate gases in a sample from each other and it is often paired with another method to detect the gases.

One method that is often combined with GC is the thermal conductivity detector, TCD, used by Golubkov et

al. [12], which uses that all gases have different thermal conductivity. The TCD has two cells with a specific temperature and a resistance that is temperature sensitive. One cell has a reference gas while the other gets the sample. The sample has a different conductivity, which changes the resistance which is measured.

The last method mentioned in this review and used by Sturk et al. 2018 [9] is a method called the wash bottle method. While the study does not dive deeper into this method, context seems to indicate that this method is based on leading the sample gas through a liquid. Some of the compounds in the sample gas will then dissolve into the water and the concentration of the compounds can then be measured. Sturk et al. 2018 [9] used a liquid that fluorine-ions could dissolve in and, assuming that the ions came from HF, the concentration of HF could then be found.

2.2.2 Composition of vented gases

A summary of the results found by the studies that measured the released gases after a thermal runaway are presented in Table 1. Sturk et al. 2019 [9], Larsson et al. 2018 [10] and Fernades et al 2018 [11] found carbonates in the gases that escaped after a thermal runaway. This group of molecules contain a carbon atom bound to three oxygen atoms. It is double bound to one of them, while the other two are bound to hydrocarbon chains. The studies detected dimethyl carbonate, DMC, diethyl carbonate, DEC and methyl ethyl carbonate, EMC. The molecular structure of DMC can be seen in Figure 3. Larsson et al. 2018 also found ethylene carbonate, EC, which is like DMC, but with the methyl-groups bound together, and ethyl acetate, EA, which is the ester version of EMC (i.e. missing one of the three oxygen atoms and therefore no carbonate). Sturk et al. 2019 found propylene carbonate, PC, which is like EMC, but the methyl-group has bounded to the ethyl–group. these compounds are often used as the electrolyte in the battery. All three studies also found HF and either POF_3 or PF_3 although Sturk et al. 2019 was not conclusive in its POF_3 finding. HF is an interesting compound because of its toxcicity, while POF_3 is of interest as it has been proposed to be a intermediate in the formation of HF [9].

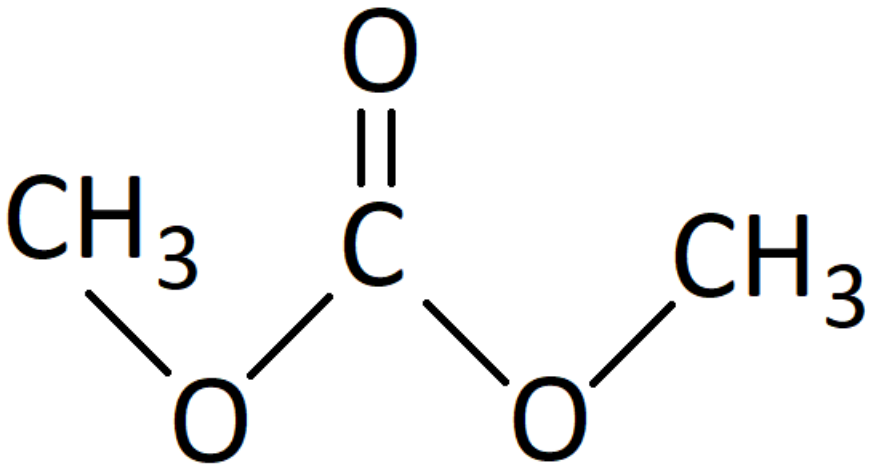

Figure 3: The molecular structure of DMC

Of these three studies, Fernades et al. 2018 was the only one that gave quantitative measurements of the mixture composition, which can be used as starting point for the simulations in the present project. They presented two mixture compositions, one where they measured the end products after the thermal runaway had completed and one where they add all of the DMC, EMC and HF measured during their continuous measurements to the end measurement. The other two studies could not be used to determine gas mixtures in the present project as Sturk et al. 2019 used the FID measurements to get the quantity of hydrocarbons and not the exact amounts of each compound. Larsson et al. 2018 studied the effect of aging on the batteries and did therefore not provide any exact measurements of the composition. It should also be noted that

Larsson et al. 2018 did not prevent fire and most of the batteries caught fire to some extent or exploded.

Golubkov et al. 2014 [12] and Yuan et al. 2020 [13] both used GC to detect and measure the gases from a battery after thermal runaway. They found a similar composition and did not detect any of the carbonates. This is not a major contradiction as Golubkov et al. 2014 calibrated their GC to detect the species they found and it is specifically mentioned that their setup could not detect HF. Yuan et al. 2020 did probably also not look for carbonates, which may explain why they were not found. Golubkov et al. 2014 and Yuan et al. 2020 got similar results. Ethylene was more common than ethane and the most abundant species were CO_2, CO and H_2. Thought it is interesting to notice that while the amount of Co_2 and CO varied drastically between the different batteries and measurements, their combined amounts are between 30% and 60% in all measurements.

Several of the already mentioned studies also measured the temperature. This was generally done in two ways, either by measuring the temperature of the batteries during the thermal runaway or by measuring the temperature of the gases after they have been released from the battery. Yuan et al. 2020 measured peak gas temperatures of 240–300 °C. The peak battery surface temperatures had a larger range, in that the NMC batteries had peak surface temperatures of 800 °C and 1000 °C, while the LFP and LTO batteries had temperatures of 400 °C and 300 °C. However, it should be noted that the thermal runaway was triggered through heating and that it happened at temperatures of 140–200 °C. Golubkov et al. 2014 also made similar observations: the battery surface for the LFP type reached roughly 400 °C, the NMC battery reached close to 700 °C and the LCO/NMC reached close to 900 °C. The gases realeased from the NMC battery had a peak temperature of 200 °C.

2.2.3 Composition of combustion products

Measurements have also been done on batteries that have been set on fire or where the gases expelled after a thermal runaway has caught fire. A summary of their results can be seen in Table 2. It should be noted that Larsson et al. 2018 is in both tables as they did not prevent the batteries from catching fires. A difference between Larsson et al. 2018 and Larsson et al. 2017 is that the earlier study was more geared towards the emission of fluorinated compounds, while the later was more about explosions in batteries and how this is affected by the aging of the batteries. The study of Truchot et al. 2018 [15] differs from the others in that it studied fires in cars and not specifically in the batteries. It is therefore not surprising they find species not found in any other study. Lecocq et al. 2016 studied the toxicity of burning batteries and did not put much focus on the fluorinated compounds. This might be the reason for why it was the only study to detect SO_2. One compound that was found in all four studies presented in Table 2 is HF.

2.3 Combustion simulations

The combustion process is a complicated chain of chemical reactions. What reactions are important in any given combustion process is a complex question. The reason for this is that the reactions involved will vary based on the fire source and the importance of any given reaction is based not only on the conditions for the combustion process, but also on other reactions. One reaction can be important for one process, but not for another because a second reaction used all of the reactants. The concentration of the reactants and the products for all of the reactions will be different for the two combustion processes. Furthermore, the concentration of the species involved will also change during the combustion. As such, combustion processes are usually characterized by different macroscopic properties. In this project two such properties will be used, the ignition delay time and the flame propagation speed. These two properties are used as one important goal of research in this field is to create safer batteries. The ignition delay time is important as it describes how the combustion of the mixture starts and simulations made to find the ignition delay time can also find information about which reactions are important for the ignition. This is important to create batteries that are less likely to catch fire. The flame propagation speed gives information on how the flame will spread after the ignition and is important to know if one wants to create batteries with less catastrophic

Table 1: Previous experimental studies of thermal runaway in batteries, summarizing what gases were found, the type of abuse that was used to trigger the thermal runaway, the detection method and what type of battery was used. The amount of each specie (in %) is indicated in parenthesise after each species. Compounds that was not conclusively detected are put in square brackets.

Study	Type of abuse	Analysis method	Battery	Species found (amount [%])
Sturk et al. 2019 [9]	Thermal	FID, FTIR, wash bottle, GC-MS	LFP, NM-C/LMO	DMC, EMC, DMC, PC, HF, [POF_3], CO_2, [CO]
Larsson et al. 2018 [14]	Thermal	FTIR	LCO	DMC, EA, EC, HF, POF_3, CO
Fernandes et al. 2018 [11]	Overcharge	FTIR	LFP	DMC (42), CO_2 (18), EMC (17), H_2 (9), C_2H_4 (3.9), CO (1.9), C_2H_5F (1.8), HF (1.3), CH_3OCH_3 (1.2), CH_3OCHO (0.8), CH_4 (0.6), CH_3F (0.4), C_2H_5OH (0.4), C_2H_6 (0.2), PF_3 (0.2), CH_3OH (0.1), C_3H_6 (0.1)
				CO_2 (47), H_2 (23), C_2H_4 (10), CO (4.9), C_2H_5F (4.6), CH_3OCH_3 (4.4), CH_3OCHO (1.9), CH_4 (1.5), C_2H_5OH (1.1), CH_3F (0.9), C_2H_6 (0.6), PF_3 (0.4), C_3H_6 (0.3), CH_3OH (0.3)
Golubkov et al. 2014 [12]	Thermal	GC-TCD	LFP	CO_2 (53.0), H_2 (30.9), C_2H_4 (6.8), CO (4.8), CH_4 (4.1), C_2H_6 (0.3)
			NMC	CO_2 (41.2), H_2 (30.8), CO (13.0), C_2H_4 (8.2), CH_4 (6.8)
			LCO/NMC	H_2 (30.0), CO (27.6), CO_2 (24.9), CH_4 (8.6), C_2H_4 (7.7), C_2H_6 (1.2)
Yuan et al. 2020 [13]	Thermal	GC	LFP	CO_2 (25.39), H_2 (24.34), CH_4 (5.9), CO (4.5), C_2H_4 (3.26), C_2H_6 (1.29), C_2H_2 (0.08)
			LTO	CO_2 (37.6), H_2 (8.41), CO (5.3), C_2H_4 (1.38), CH_4 (1.23), C_2H_6 (0.4), C_2H_2 (0.0008)
			NMC	CO (30.3), CO_2 (13.22), H_2 (12.39), CH_4 (10.5), C_2H_6 (0.16), C_2H_4 (0.1), C_2H_2 (0.0026)
			NMC	CO (28.06), CO_2 (19.91), CH_4 (12.9), H_2 (12.54), C_2H_6 (0.21), C_2H_4 (0.16), C_2H_2 (0.0027)

combustion accidents. The ignition delay time and the flame propagation speed are both dependent on the starting composition of the mixtures and they can be studied both through computer simulations and physical experiments.

The complexity of the combustion process has some implications for the simulation run time. As is common for computer simulations, the time it takes to run a simulation increases strongly with the complexity of the simulation. This means that much time can be saved if it is possible to reduce the complexity of the simulation. One method to do this is to reduce the dimension of the simulation. This simplifies the simulation by reducing the size of the system and by reducing the complexity of processes such as diffusion and turbulence [17]. Though, the simulations done in this project have been simplified as to not contain any turbulence. While three-dimensional simulations can simulate entire flames, one-dimensional simulations can determine specific properties of the flame and this reduce the simulation time. This is one of the reasons why this

Table 2: Previous experimental studies of batteries that have caught fire or have exploded. The table summarizes what gases have been found in experimental studies, as well as what type of abuse was used to trigger the thermal runaway and fire, the detection method and what type of battery was used.

Study	Type of abuse	Method	Battery	Species found
Larsson et al. 2017 [10]	External Fire	FTIR	LFP, LCO	HF, POF_3
Larsson et al. 2018 [14]	Thermal	FTIR	LCO	EA, DMC, EC, CO, HF, POF_3
Truchot et al. 2018 [12]	External Fire	NDIR, FTIR, FID	Entire car	CO_2, CO, HF, HCl, HCN, NO, NO_2
Lecocq et al. 2016 [9]	Thermal	NDIR, FTIR, FID	LFP	CO, HF, SO_2

project was performed with one-dimensional simulations.

Another source of complexity is the kinetic mechanism used in the simulation. Kinetic mechanisms fall into different categories depending on the complexity. The most complex is the complete mechanisms that contains all of the reactions and species involved in the combustion. The simplest version is called a global or single-step mechanism and may contain only one reaction. An example of such a reaction is seen when DMC reacts with oxygen to produce water and carbon dioxide:

$$CH_3OCOOCH_3 + 3O_2 \rightarrow 3H_2O + 3CO_2 \tag{1}$$

Semi-global mechanisms are a bit more complex and typically contains 4–10 species [17]. In between complete and semi-global mechanism lies detailed and skeletal mechanisms. Skeletal mechanisms contain only the main reactions used in the combustion, while a detailed mechanism usually contains most reactions involved in the combustion of the fuel. The length varies greatly based on complexity and the fuel. The Lawrence Livermore national Laboratories, LLNL, have presented a mechanism for heptane combustion containing 561 species and 2539 reactions [19], while detailed hydrogen combustion mechanisms usually contain only 8 species. [17]

2.4 Chemical kinetics

A stoichiometric equation is an equation that shows how much of the reactants are required to create the products. An example is when ethylene reacts with hydrogen gas to form atomic hydrogen and an ethyl radical:

$$C_2H_4 + H_2 \rightleftharpoons H^\bullet + C_2H_5{}^\bullet \tag{2}$$

The superscript dot for the atomic hydrogen and the ethyl radical indicate that these species are radicals. A radical is a atom or molecule that contains unpaired electrons and they are therefore very reactive. The reaction is reversible and that is indicated by the $\rightleftharpoons$ symbol. A reversible reaction is a reaction where the products can react and create the reactants. An irreversible reaction is indicated by an arrow pointing in only one direction and Eq. 1 shows such a reaction. It is possible to have three reactants in a reaction, but that requires all of the species to collide in a short span of time and are therefore usually less likely. The rate for three-body reactions typically increases with pressure.

Termolecular is a special kind of reaction, which involves an unspecified molecule M that is not consumed by the reaction. In such a reaction, two specified species first collide and react, forming a product in an excited state that normally spontaneous fall apart. However, this can be prevented when the product collides with M, passing its surplus of energy to M [21]. An example of this kind of reaction is given by

$$C_2H_3 + H + M \rightleftharpoons C_2H_4 + M \tag{3}$$

The speed of a reaction is quantified by the reaction rate, r [20], which is defined as

$$r = \frac{1}{s}\frac{dS}{dt} \tag{4}$$

where s is the stochiometric coefficient, S is the concentration of the species and t is the time [20]. The reaction rate does not depend on which species one uses for the formula. It only depend on the reaction. That is why one can use a rate constant, k, for the reaction to calculate r [22]. r can be approximated with the equation

$$r = k\prod S_i^{c_i} \tag{5}$$

where S_i is the i:th species and c_i is a positive real number or zero [20]. This shows a clear difference between two- and three-body reactions in combustion processes as the concentration of gases are typically quite low. k typically have a temperature dependence and that can be described by the Arrhenius equation:

$$k = Ae^{-\frac{E_A}{RT}} \tag{6}$$

where T is the temperature, E_A is the activation energy, R is the gas constant and A is a constant depending on the reaction. The Arrhenius equation has been modified for high temperature gas-phase kinetic systems to better describe the temperature dependence of k. Combustion processes usually reach high temperatures and many species are in tha gas phase. Combustion mechanisms therefore typically use the modified Arrhenius equation [22]:

$$k = AT^n e^{-\frac{E_A}{RT}} \tag{7}$$

where n is another reaction-specific constant.

Three constants, E_A, n and A, are therefore used to describe every reaction in the mechanism. These are then used during the simulation to find the reaction rate of each reaction. Eq. 4 is a differential equation for how the concentration of one species changes with time. A similar equation exists for every species in the reaction mechanism. This system can be solved by starting from a specified composition (concentration of all reactants) and taking small time steps, changing the concentrations according to the differential equations. This continues for a user-specified amount of time. Such a simulation can be used to find the ignition time of the combustion. The system could be imagined as a ball of fuel and oxidizer perfectly mixed at a certain starting temperature. The reactions will happen and energy will be released. This will increase the temperature, which will increase the rate of most of the reactions. This will continue until all of the fuel is consumed. As the combustion process is a chain of reactions, there is no absolute marker that one can use to find the specific time at which the fire started. The definition used in this project is that the ignition time is the time from the start of the simulation to the maximum change in temperature is achieved. Another common definition is to use the peak concentration of hydroxide radical.

The kinetic equations above only consider time, but no spatial coordinates. Alternetivly, the spatial propogation of the reactions can also be studied. An example of a simulation that does not use time steps is the simulations used to find the laminar flame speed of the combustion. Laminar flame speed is the speed at which the flames propagate through a motionless, homogeneous mixture of fuel and oxidizer. One could imagine a tub filled with the mixture. The mixture is set ablaze at one end and one measures how long it

takes for the flame front to travel a certain distance. From that one can calculate the speed. Another method is to create a laminar flow at a certain speed and ignite it. If the laminar flame speed is different from the flow speed, then the flame front will move compared to the flow. The laminar flame speed can be found by changing the flow speed until the flame front does not move relative to the flow. This is similar to what the simulation does, except it uses thermodynamic equations to find the equilibrium.

3 Methods

The aim of this study is to investigate how the composition of a gas mixture typical for thermal runaway in batteries affects the propensity of the mixture to ignite and the flame to propagate. Our target has been the the type of gas mixtures presented in Table 1, but we have used simpler mixtures to reveal the impact of the different components.

Roughly 250 simulations have been performed differing in the simulation type, the mechanism used and the gas mixture used. The simulation type determines the system simulated and what information the simulation gives. The mechanism determines the chemistry considered and the gas mixture determines what compounds are studied.

3.1 Simulations

Two different types of simulations were performed using the software Chemkin [26]. The first was a one-dimensional system in which the system can propegate from a gas inlet, to the product exit. This configuration was used for the flame speed simulations. The gas pressure was 1 atm and the starting gas temperature was 300 K, which is close to room temperature. The simulations employed 750 grid points. No grid independence study was performed, but previous experience has shown that this grid is sufficient for this type of simulations. The axis length was 5 cm and the oxidation source was air, $N_2(0.79)$ and $O_2(0.21)$. The simulations were done for 10 equivalence ratios starting from 0.1 and ending in 1.9 with steps of 0.2. The wide variation in the equivalence ratio was chosen as the gases released from a thermal runaway starts concentrated and then are diluted as they spread. For all other parameters, Chemkins default settings were used.

The second simulation setup only had one component, a closed homogeneous gas mixture, and it was used to find the ignition delay time. The oxidation agent was air and three equivalence ratios of 0.7, 1.0 and 1.3 were investigated. The simulations were performed at 9 initial temperatures starting at 700 K and ending at 1500 K with steps of 100 K. These temperatures were chosen based on the surface temperatures of the batteries and the self-ignition temperatures. The end products from the combustion were N_2, H_2O, CO_2 and HF. HF was chosen based on the combustion products found in the literature [18] and the other three are standard complete combustion products.

3.2 Mechanisms

Three chemical kinetic mechanisms were used in the simulations. The first was made by Alexandrino et al. 2018 [23] with the intention of being used in combustion simulations of DMC. This is a relative new mechanism that has been developed using up to date reaction rate constants and thermodynamic data. A mechanism for DMC was chosen instead of a mechanism for some other carbonate because DMC is the smallest of the carbonates and will therefore have the lowest number of reactions in its mechanism. This decreases the simulation time while still giving results that are representative for carbonates. Another reason is that the combustion of carbonates have not been studied extensively and there are therefore not many mechanisms to choose for the carbonates. This mechanism will be referred to as DMC-mech and it has a length of 2737 reactions.

The second mechanism used was developed by Linteris et al. 2020 [24] for small fluorinated compounds. It was developed within the larger context of atmospheric research of fluorinated compounds released from refrigerators. It contains a hydrocarbon chemistry subset that is based on the older GRI 3.0 mechanism [25], which is less accurate than DMC-mech. The DMC-mech is expected to predict hydrocarbon and radical species with much higher accuracy, in particular for low temperature ignition cases. This mechanism will be referred to as F-mech and it is 101 species and 915 reactions long.

The third mechanism is a combination of DMC-mech and F-mech that will be referred to as DMC+F-mech. It was created by taking all of the subsets containing fluorine from the F-mech and inserting them into DMC-mech. One modification to the F-mech had to be done as the fluorine chemistry was extracted and coupled with the DMC-mech: In the F-mech, the radical C_3H_7 existed in one form, while in the DMC-mech it has two isomer forms. Therefore, all C_3H_7 only in the F-mech was replaced by n-C_3H_7 when coupled to the DMC-mech. The DMC+F-mech has been compared to the two other mechanisms by running simulations for the same mixtures and comparing the results.

3.3 Mixtures

The mixtures used in the simulations can be seen in Table 3 and they fall into three categories, gradually changing mixtures, literature mixtures and other. The gradually changing mixtures are simple mixtures containing one or two compounds typical for gas mixtures of vent gases from batteries that has undergone thermal runaway. If the mixtures are arranged properly they create a gradual change from one pure component to another. The compounds used in these mixtures where chosen as representatives of chemical groups. DMC represents carbonates, while C_2H_4 represents alkenes and hydrocarbons with two carbons. The literature mixtures are based on the mixtures found in Table 1 and represent real-world mixtures, but with simplifications. For example, all carbonates are represented by DMC. They were normalized to eliminate rounding errors and other unknown compounds. All compounds containing fluorine were replaced by the closest species not containing fluorine. For example, C_2H_5F was changed to C_2H_6. None of the mechanisms used contains POF_3 and it was eliminated from the mixtures. Finally, the last group contains more complex mixtures that bridges the gap between the literature mixtures and the gradually changing mixtures.

Table 3: Simulation runs, described by the name, mechanism used and the composition of the mixture.

Name	Mechanism	Mixture
DMC–C_2H_4	DMC	From pure DMC to pure C_2H_4 in 11 steps
DMC–CO_2	DMC	From pure DMC to pure CO_2 in 11 steps
DMC–CO	DMC	From pure DMC to pure CO in 11 steps
C_2H_4–H_2	DMC	From pure C_2H_4 to pure H_2 in 11 steps
DMC–H_2	DMC	From pure DMC to pure H_2 in 11 steps
DMC–H_2	DMC+F	From pure DMC to pure H_2 in 11 steps
DMC–C_2H_5F	DMC+F	C_2H_5F in DMC with (0.01, 0.05, 0.10, 0.15, 0.2) C_2H_5F
DMC–CH_3F	DMC+F	CH_3F in DMC with (0.01, 0.05, 0.10, 0.15, 0.2) CH_3F
DMC–HF	DMC+F	HF in DMC with (0.01, 0.05, 0.10, 0.15, 0.2) HF
CH_3F–HF	F	From pure CH_3F to pure HF in 11 steps
CH_3F–HF	DMC+F	From pure CH_3F to pure HF in 11 steps
Fernandes 1	DMC	See Table 1 for the composition. F-species has been replaced with closest non F-species and EMC has been replaced with DMC. PF_3 has been removed.
Fernandes 1	DMC+F	See Table 1 for the composition. EMC has been replaced with DMC and PF_3 has been removed.
Fernandes 2	DMC	See Table 1 for the composition. F-species has been replaced with closest non F-species and PF_3 has been removed.
Fernandes 2	DMC+F	See Table 1 for the composition. PF_3 has been removed.
Golubkov LFP	DMC	See Table 1 for the composition.
Golubkov NMC	DMC	See Table 1 for the composition.
Golubkov LCO/NMC	DMC	See Table 1 for the composition.
Yuan LFP	DMC	See Table 1 for the composition.
Yuan LTO	DMC	See Table 1 for the composition.
Yuan NMC 1	DMC	See Table 1 for the composition.
Yuan NMC 2	DMC	See Table 1 for the composition.
Other 1	DMC	DMC (0.8), CO_2 (0.1), H_2 (0.1)
Other 2	DMC	DMC (0.7), CO_2 (0.2), H_2 (0.1)
Other 3	DMC	DMC(0.7), CO_2(0.18), H_2(0.1), CO(0.02)
Other 4	DMC	H_2 (0.9), CH_4 (0.1)
Other 5	DMC	H_2 (0.8), CO_2 (0.1), CH_4 (0.1)
Other 6	DMC	From H_2 (0.7) and CO_2 (0.1) to H_2 (0.1) and CO_2 (0.7) in 7 steps + CO (0.1), CH_4 (0.1)
Other 7	DMC	From H_2 (0.6) and CO (0.1) to H_2 (0.2) and CO (0.5) in 5 steps + CO_2 (0.2), CH_4 (0.1)
Other 8	DMC	CO (0.4), CO_2 (0.2), H_2 (0.2), CH_4 (0.2)
Other 9	DMC	CO_2 (0.5), H_2 (0.2), C_2H_4 (0.1), CO (0.1), CH_4 (0.1)

4 Results

4.1 Ignition times

Figure 4 shows the simulated ignition delay times for pure DMC and C_2H_4 in air as a function of the starting temperature for three equivalence ratios, phi, varying from oxygen excess (0.7) to fuel excess (1.3). The temperature is given as 1000/T, where T is the temperature in K and the higher temperatures are therefore on the left side of the graph. As explained earlier in this report, DMC and C_2H_4 are suitable compounds to represent hydrocarbons in gas mixtures from batteries undergoing thermal runaway, and therefore these are relevant to compare. The ignition time is orders of magnitude longer for the lower temperatures than for the higher temperatures, while the difference between the equivalence ratios is relatively small. The effect of the increase in temperature is not the same for the two fuels. It can be seen in Figure 4 that the ignition time of C_2H_4 has a exponential temperature dependence for lower temperatures, but the dependence changes slightly for the highest temperatures. DMC, on the other hand, seems to have two different temperature dependencies for the high and low temperatures. Both are exponential, but the ignition time decreases faster for the higher temperatures than the lower temperatures.

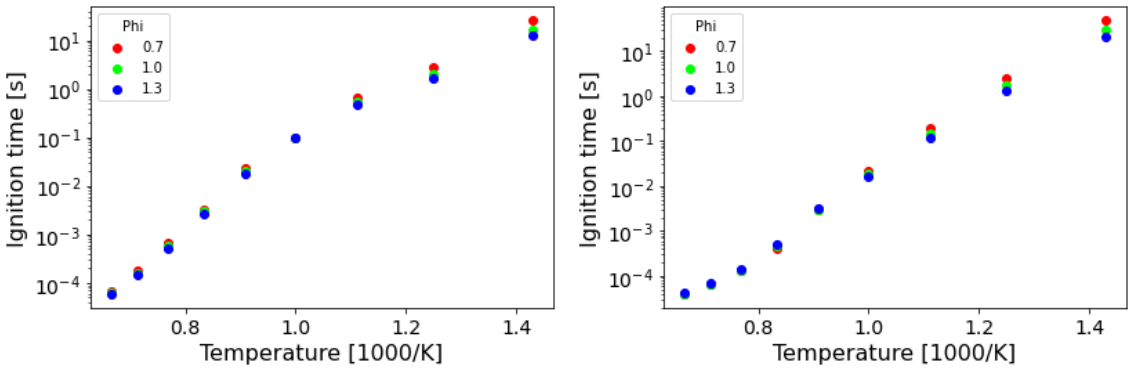

Figure 4: Ignition times for pure DMC (left) and pure C_2H_4 (right) as a function of temperature. The equivalence ratio of 0.7 is colored red, 1.0 is green and 1.3 is blue.

Many different types of batteries have been made and are commercially available. It is therefore important to find how the ignition time changes as the composition of the gas mixture changes. Figure 5 shows how the trend changes when the mixture is gradually changed from either pure DMC or C_2H_4 to pure C_2H_4 or H_2. The change in the composition causes a gradual change in the ignition time such that the ignition time goes from the ignition time for one of the pure substances to the ignition time for the other substance. This change is not linear. In the case of DMC–C_2H_4, (left panel of Figure 5), the mixture is acting more like the pure DMC than the pure C_2H_4. The difference between pure C_2H_4 and H_2 is small, but at some points, it seems that the mixture is acting slightly more like C_2H_4 than what a linear prediction would suggest. Another point of interest is that C_2H_4 has a faster ignition time than DMC for most temperatures. C_2H_4 has a slightly longer ignition time than for DMC at the lowest temperature. The ignition time for H_2 is shorter than the ignition time for C_2H_4 at higher temperatures, but longer for lower temperatures.

The gas mixtures released from batteries after thermal runaway contained both CO_2 and CO in varying proportions. It is therefore important to find how different amounts of CO_2 and CO affects the ignition time of mixtures. Figures 6 and 7 show how the ignition time of a mixture changes as DMC is diluted with CO_2 or CO. The DMC mixture, Figure 6, does not show any significant changes in ignition delay time when diluted with either CO_2 or CO. The exception is pure CO which diverges from all of the other mixtures. However, the mixtures in figure 7 show a great change. The ignition time is drastically increased by one order of magnitude when the amount of CO_2 is increased in the primarily H_2 mixture. A similar increase can be seen when the amount of CO is increased.

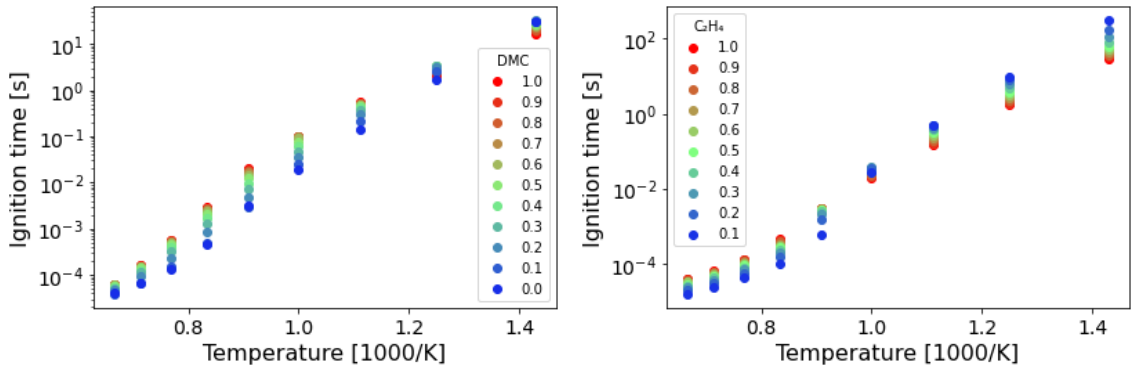

Figure 5: Ignition times for the DMC–C_2H_4 mixtures (left) and C_2H_4–H_2 mixtures (right) as a function of temperature. The equivalence ratio is 1.0. Pure DMC (left) and pure C_2H_4 (right) is represented with red and the color changes from red to green and then to blue as the mixture contains more C_2H_4 (left) or H_2 (right).

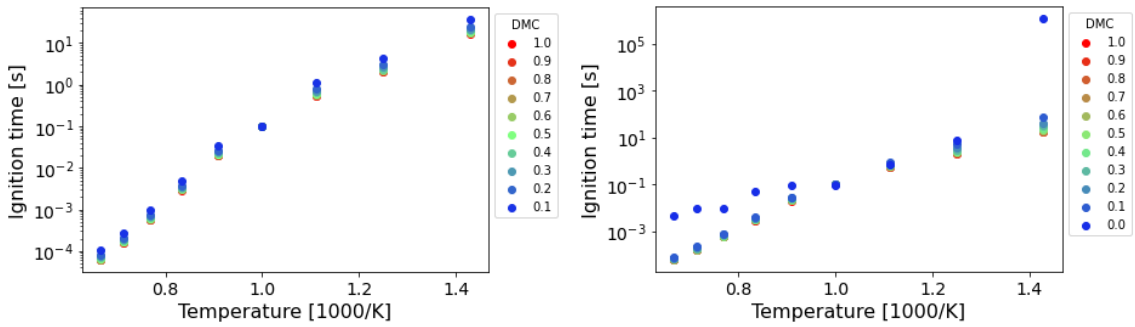

Figure 6: Ignition times for the DMC-CO_2 (left) and DMC-CO mixtures (right) as a function of temperature. All results are for the equivalence ratio of 1.0. Pure DMC is represented with red and the color changes from red to green and then to blue as the mixture contains more CO_2 (left) or CO (right).

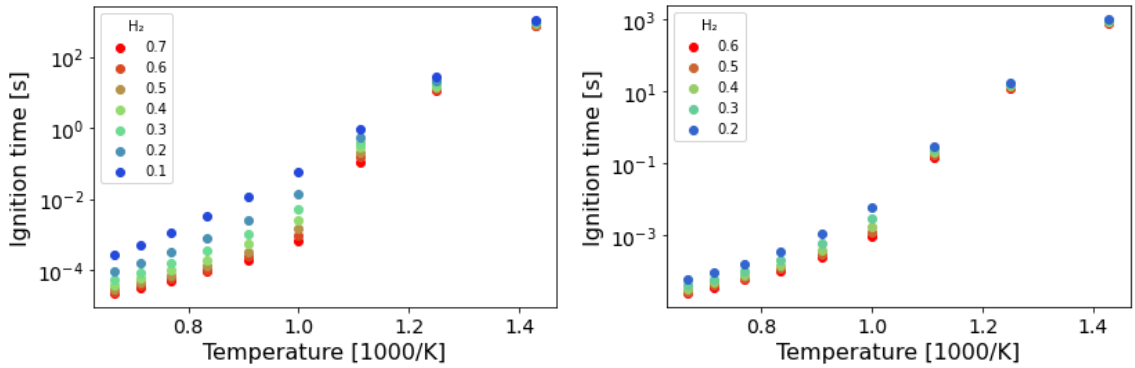

Figure 7: Ignition times for the Other 6 (left) and Other 7 mixtures (right) as a function of temperature. All results are for the equivalence ratio of 1.0. Mixtures containing more H_2 is represented with red and the color changes from red to green and then to blue as the mixture contains more CO_2 (left) or CO (right).

What made battery fires different from fires in other fields of research is that they contain fluorinated compounds. As such, it is important to find how the introduction of fluorinated compounds changes the ignition delay time. Figure 8 shows how fluorinated compounds change the ignition time of DMC. The

compounds did generally not have any significant effect on the ignition time. The two lowest temperatures show a small variation from the pure DMC mixture.

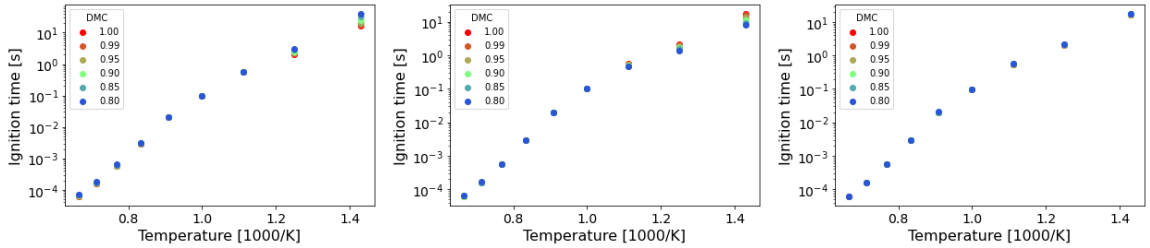

Figure 8: Ignition times for DMC–C_2H_5F (left), DMC-CH_3F (middle) and DMC-HF mixtures (right) as a function of temperature. All results are for the equivalence ratio of 1.0. Pure DMC is represented with red and the color changes from red to green and then to blue as the mixture contains more C_2H_5F (left), CH_3F or HF (right).

The ignition time for mixtures that were based on real measurements can be seen in figure 9. The different simulations found different ignition times for the batteries of the same types. The difference between the Fernandes mixtures is if they contain DMC, 1 has, and if they contain fluorinated compounds, DMC+F-mech has. All four diverge at lower temperatures, but the fluorinated compounds do not change the ignition delay time at higher temperatures. Golubkov LFP and Yuan LFP are both based on measurements from the same type of battery as the Fernandes mixture. The Fernandes mixtures had smaller ignition delay times than the Golubkov LFP and the Yuan LFP, but their mixtures got similar results. However, their NMC mixtures got different ignition times. The Golubkov LFP and NMC, and Yuan LFP and LTO mixtures were dominated by CO_2 and H_2 as second, while the Golubkov LCO/NMC mixture had H_2 as its most abundant component with CO coming second. The Yuan NMC 1 and 2 mixtures was dominated by CO and CO_2.

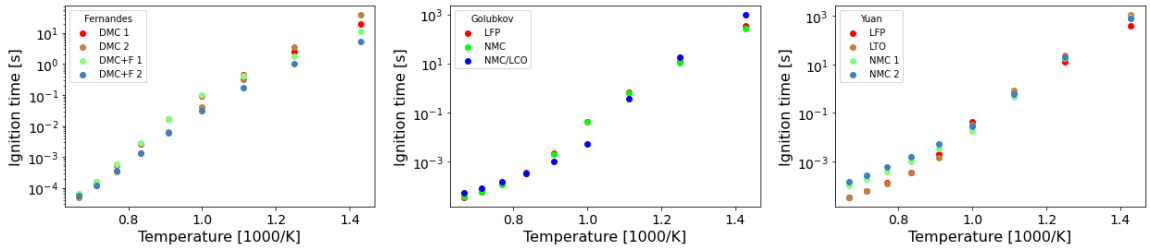

Figure 9: Ignition times for the Fernandes mixtures (left), Golubkov (middle) and Yuan mixtures (right) as a function of temperature. All results are for the equivalence ratio of 1.0.

It can be seen in figure 10 and 11 that DMC+F-mech gave slightly different values than DMC-mech and F-mech. The relative difference has been calculated by taking the difference in ignition time between DMC-mech or F-mech, and DMC+F-mech and then divide the difference with the DMC-mech or F-mech values. This is done to find how the DMC+F-mech differs from the mechanisms used to construct it. DMC+F-mech contains the fluorine part of the F-mech and is therefore expected to act like F-mech when used on a mixture that only contains fluorinated compounds. All of the pure hydrocarbon chemistry comes from DMC-mech and DMC+F-mech should act like DMC-mech when there are no fluorinated compounds in the mixture. The expected difference on the ignition time for the same pure mixture either only containing or not containing fluorinated compounds is zero. The difference is divided with the value from the DMC-mech or the F-mech because of the large span of values for the ignition delay time. A doubling is significant for any temperature, but an increase of 1 ms is not significant for the lower temperatures. The relative difference was not zero for all mixtures and temperatures. High temperature had a wide spread on the relative difference for the DMC–H_2 mixtures, but no trend can be seen. The CH_3F–HF mixtures had negative relative differences for high temperatures and positive relative differences for low temperatures.

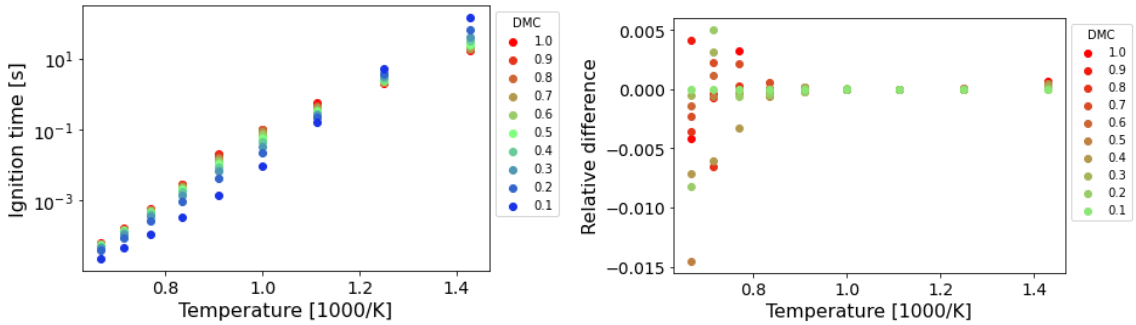

Figure 10: Ignition times for the DMC–H_2 mixtures (left) for the equivalence ratio of 1.0 when the DMC mechanism was used. The figure to the right shows the relative differencein the ignition time obtained from simulations using DMC-mech or DMC+F-mech. Pure DMC is represented with red and the color changes from red to green and then to blue as the mixture contains more H_2

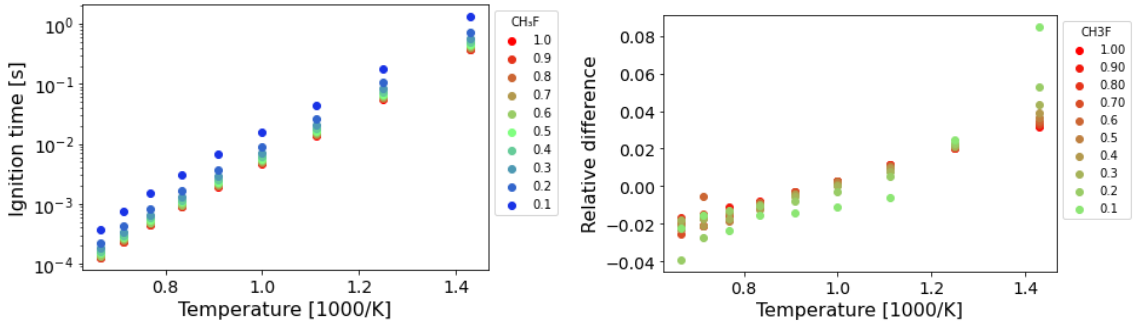

Figure 11: Ignition times for the CH_3F–HF mixtures (left) for the equivalence ratio of 1.0 when the F mechanism was used. The figure to the right shows the relative difference in the ignition time obtained from simulations using DMC-mech and DMC+F-mech. Pure CH_3F is represented with red and the color changes from red to green and then to blue as the mixture contains more HF

4.2 Flame speed

The simulations done for equivalence ratios of 0.1 and 0.3 failed for most mixtures and have therefore been excluded from all results presented here. The reason for this is that these equivalence ratios has very low flame speeds. This also makes them hard to measure, as they do not always catch fire, and the simulations can therefore not be compared to experimental values. A few additional equivalence ratios also failed seemingly without any pattern and those have also been left out. It is expected to have been caused by numerical difficulties for the software with the convergence to an answer. The flame speed found for pure DMC and C_2H_4 can be seen in figure 12. Both shows a maximum around the equivalence ratio of 1.1. Pure C_2H_4 gave flame speeds that were roughly twice as high as the flame speeds of pure DMC, which is in line with the experimental results seen for these fuels [23].

It can be seen in figure 13 that the flame speed varies with the mixture. The DMC–C_2H_4 mixtures have a close to linear relation between mixture composition and the flame speed, while the C_2H_4–H_2 mixtures have a clearly non-linear relation between the mixture composition and the flame speed. The trend for hydrocarbons mixed with H_2 is that hydrocarbons dominate the mixture until the amount of H_2 reaches roughly 60% where the H_2 starts to dominate.

The effect on the flame speed of adding CO_2 or CO to a mixture can be seen in Figures 14 and 15. The addition of CO_2 has a clear slowing effect on the flame speed with the flame speed going to zero as the concentration of CO_2 increases. The effect of adding CO to a mixture changes the flame speed to act more

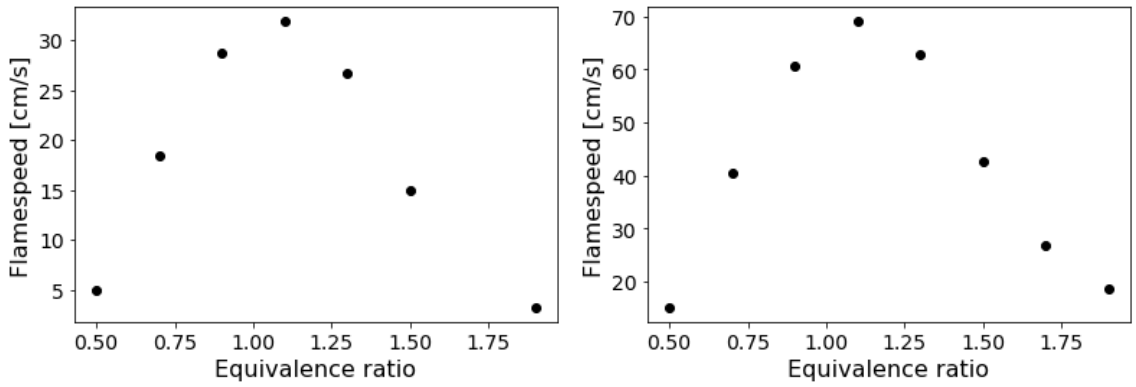

Figure 12: Flame speeds for pure DMC (left) and pure C_2H_4 (right) as a function of equivalence ratio.

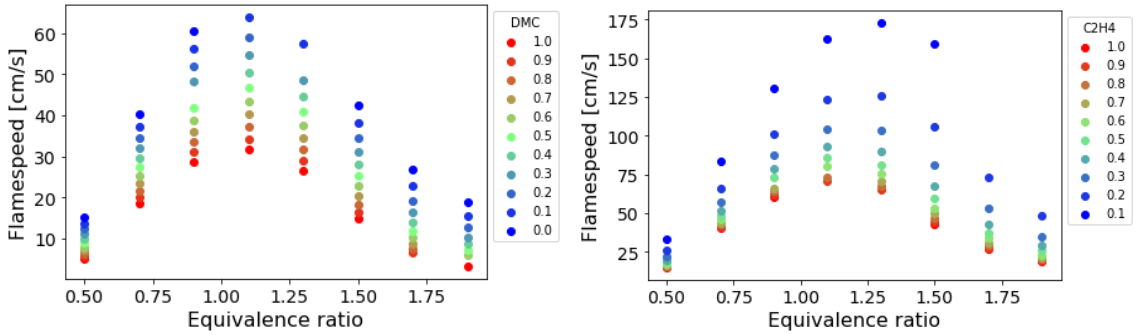

Figure 13: Flame speeds for the DMC–C_2H_4 (left) and C_2H_4–H_2 mixtures (right) as a function of the equivalence ratio. Pure DMC (left) and pure C_2H_4 (right) is represented with red and the color changes from red to green and then to blue as the mixture contains more C_2H_4 (left) or H_2 (right).

like pure CO. The peak flame speed of mixtures with CO is moved from the equivalence ratio of 1.1 to 1.5.

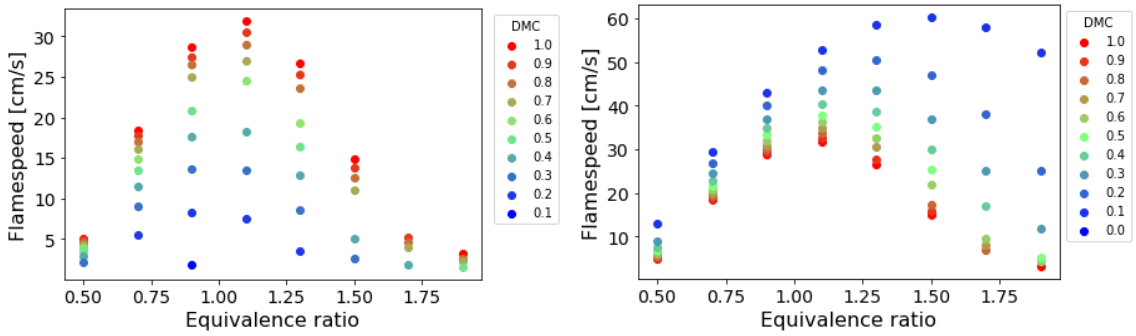

Figure 14: Flame speeds for the DMC–CO_2 (left) and DMC–CO mixtures (right) as a function of equivalence ratio. Pure DMC is represented with red and the color changes from red to green and then to blue as the mixture contains more CO_2 (left) or CO (right).

The addition of species containing fluorine had little effect on the flame speed of the mixture. This can be seen in figure 16 where the flame speeds of the different DMC mixtures containing C_2H_5F, CH_3F or HF has been plotted. This can also be seen in figure 17 where the flame speeds from the mixtures that were taken from the literature are shown. The flame speeds from the Fernandes mixtures show little difference between the mixtures containing fluorinated compounds or not. A clear difference between the different battery types

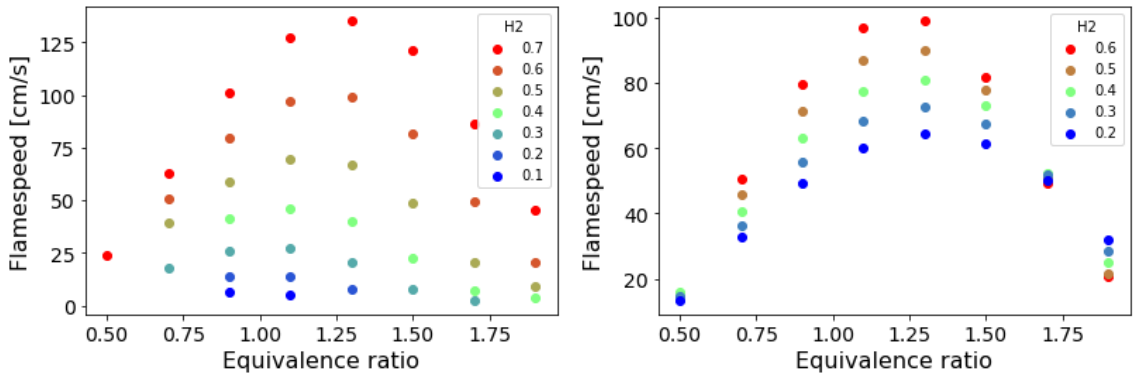

Figure 15: Flame speeds for the Other 6 (left) and Other 7 mixtures (right) as a function of temperature equivalence ratio. Mixtures containing more H_2 is represented with red and the color changes from red to green and then to blue as the mixture contains more CO_2 (left) or CO (right).

can be seen both for the Golubkov and the Yuan mixtures. However, Yuan LTO contained a large amount of CO_2 and failed to run.

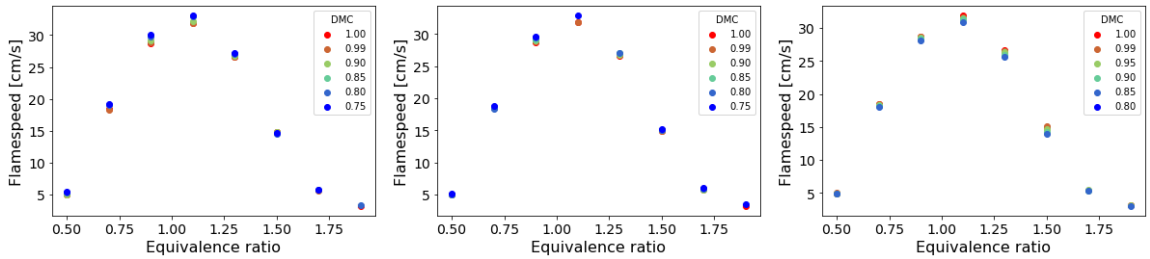

Figure 16: Flame speeds for the DMC–C_2H_5F (left), DMC–CH_3F (middle) and DMC–HF mixtures (right) as a function of equivalence ratio. Pure DMC is represented with red and the color changes from red to green and then to blue as the mixture contains more C_2H_5F (left), CH_3F or HF (right).

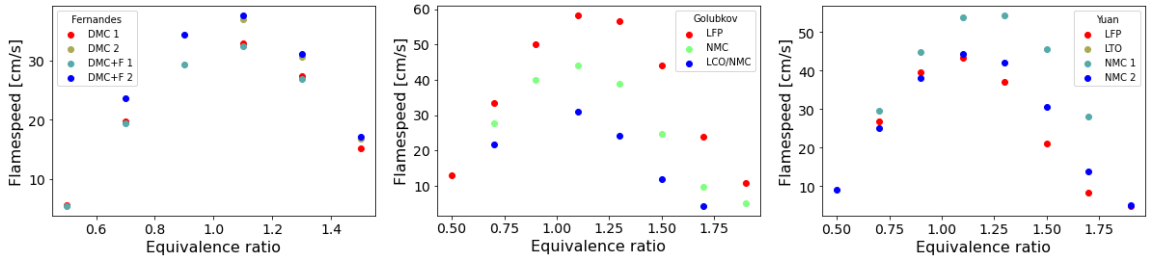

Figure 17: Flame speeds for the Fernandes (left), Golubkov (middle) and Yuan mixtures (right) as a function of equivalence ratio.

The relative difference between the original mechanisms and the combined mechanisms can be seen in figures 18 and 19. The relative difference has been calculated by taking the difference in flame speed from the mixtures when DMC-mech or F-mech were used compared to the DMC+F-mech and then dividing this with the value of the flame speed for the DMC-mech or the F-mech. This was done to find how the DMC+F-mech varies compared to the DMC-mech or F-mech. The relative difference is small for the DMC–H_2 mixtures, where it randomly varies without any discernible trend for either temperature or mixture composition. A clear trend can be seen in the relative difference for the CH_3F–HF mixtures, where higher temperatures have negative values and lower temperature have positive values.

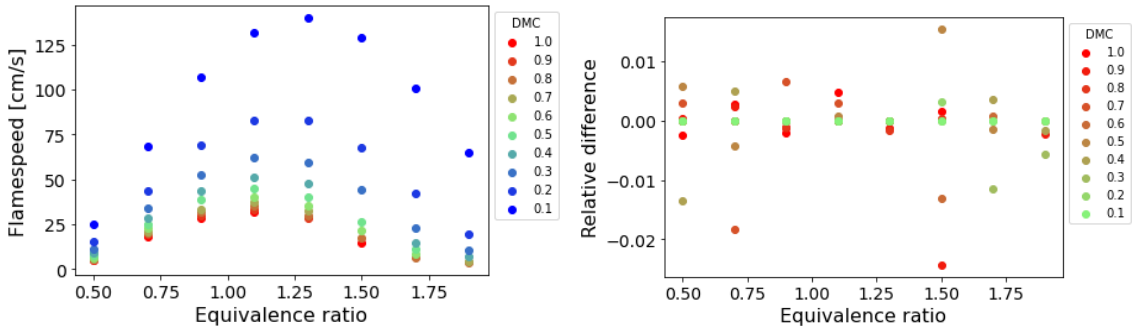

Figure 18: Flame speeds for the DMC–H_2 mixtures (left) when the DMC mechanism was used. To the right is the relative difference between the DMC and DMC+F mechanisms fort the DMC–H_2 mixtures. Pure DMC is represented with red and the color changes from red to green and then to blue as the mixture contains more H_2.

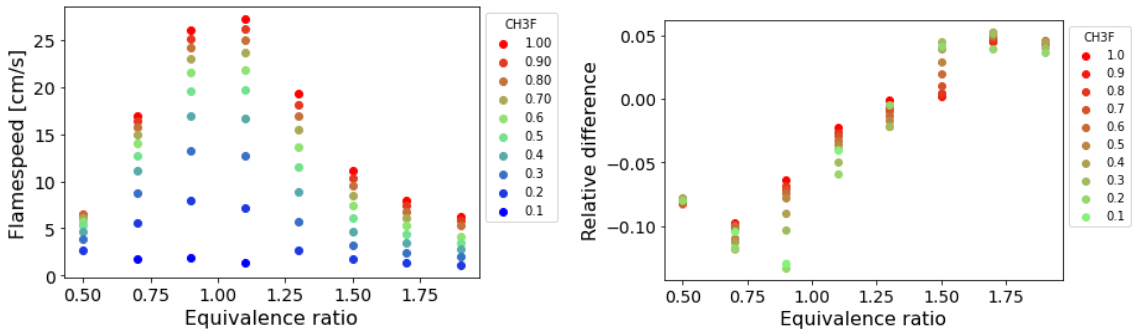

Figure 19: Flame speeds for the CH_3F–HF mixtures (left) when the F mechanism was used. To the right is the relative difference between the F and DMC+F mechanisms for the CH_3F–HF mixtures. Pure CH_3F is represented with red and the color changes from red to green and then to blue as the mixture contains more HF.

5 Discussion

5.1 Ignition time

It is clear from the simulations that the largest factor in the determination of the ignition time is the temperature. At low temperatures it takes sometimes thousands of seconds before the mixture ignites, while the ignition time for the high temperatures were only tens of μs. This finding is expected as the rate constants have an exponential dependence on the temperature, as can be seen from the modified Arrhenius equation (Eq. 7). Increasing the temperature is therefore expected to increase the reaction rate. Compared to the temperature, the equivalence ratio of the mixture had a small effect. It might seem strange that changing the amount of fuel compared to the oxygen in the mixture will not have any significant effect, but the reason for this might be that the ignition time is mainly dependent on the starting reactions of the combustion. In the start of the combustion, both the oxygen and the fuel is in a relative stable form and the first couple of reactions will break the molecules into radical pieces. An example of such a reaction is shown in Eq. 3, where ethylene collides with some other species to loose one of its hydrogen. This reaction is independent of the nature of the other species and will therefore only be affected by the concentration of the fuel and the temperature. It is quite common for the starting reactions to be like that and it is not until later when the first reactions have created radicals that the reactions with more specific reactants start. To confirm this one would need to analyse which reactions are important for the ignition of the fuel. It can be done in Chemkin,

but there were not enough time to do this in this project.

The ignition time for the gradually changing mixtures where sometimes affected by the change in the mixture, sometimes not. The general trend seems to be that any two-component mixtures will have an ignition time somewhere in between the ignition time of the pure components. One could have imagined that the component with the fastest ignition time would dominate the mixture. It would do that by igniting quickly and then help the ignition of the other parts of the fuel. Another hypothesis is that there would be a linear relation between the ignition time and the mixture composition, such that a mixture of equal amount of two components would have an ignition time that is the average of between that of the two components. Neither of these hypothesis turned out to be true, with one exception. The exception is when the ignition time is orders of magnitude larger for one specie than another and the mixture will then be dominated by the specie with the faster ignition time. Otherwise, the ignition time for a mixture of two components is somewhere in between the ignition times of the pure components, but it is not possible to predict where. Figure 15 shows that the mixtures with relative high concentration of H_2 have much more similar ignition times than the mixtures with low concentration of H_2. In the DMC–C_2H_4 mixture, see Figure 13, a similar trend for DMC can be seen. The difference is that DMC has a longer ignition time than C_2H_4, while H_2 is the component with the fastest ignition time in this study.

The reason why the DMC–CO_2 mixture did not show any changed ignition times could have a similar explanation as why the ignition time did not change with the equivalence ratio. However, this does not explain why the Other 6 mixtures showed changed ignition time. It could be that a methane and carbon monoxide have a very long ignition time compared to hydrogen and that the Other 6 mixture was moving towards an ignition time of that mixture as the hydrogen was removed. This seems unlikely as the ignition time of the mixture is much slower than the ignition time of CO and H_2. If methane also followed the same trend seen for DMC, C_2H_4 and H_2, and the longer ignition times were caused by methane, then it would have an ignition time that is multiple orders of magnitude lower than all of the other compounds that have been studied in this project. While this can't be ruled out based on this study, methane is not properly represented by any of the other compounds as it is an alkane with only one carbon. The author of this report would find it surprising if this turned out to be the correct explanation. Another explanation is that, while DMC relies on termolecular reactions to start, hydrogen might not and this could mean a different dependence on the concentration.

It might seem strange that the DMC–CO mixture was unaffected by a change in the composition, but if DMC relies on termolecular reactions to start then it is not starnge that the amount of CO does not affect the ignition delay time. The ignition delay time for the pure CO is different in that it is not strictly decreasing as the temperature increases. The reason for this is probably that different reactions dominate at different temperatures and the reactions have different temperature dependencies. It is also noteworthy that CO has an extremely long ignition time compared to most other compounds in this study. This indicates that CO is a relative stable compound at low temperature.

The fluorinated compounds did not change the ignition time of DMC in any noteworthy way. This is strange as most other compounds, to some extent, changed the ignition time of the mixture as their concentration is changed. The total amount tested is different for the fluorinated compounds than for the other gradually changing mixtures and the reason for this is that the amounts of fluorinated compounds vented after a thermal runaway found in the literature are much smaller than for most other compounds tested here. The ignition time of methyl fluoride is lower than for most other compounds tested in this study, but not much lower. This can be seen if one compares figure 11 to Figure 13. Hydro fluoride should have a similar effect on mixtures as carbon dioxide as both are complete combustion products.

The fluorinated compounds did not have any significant effect on the ignition rate of the Fernandes mixtures either. Including or excluding DMC, on the other hand, had an effect on the ignition time of the mixture. The Golubkov LFP and NMC, and Yuan LFP and LTO mixtures had similar ignitions times and compositions. The Yuan NMC 1 and 2 mixtures had ignition times that were similar, while the Golubkov NMC/LCO mixture was different from the others. This means that the mixtures does not group together based on the type of the battery, but based on the composition of the gases released after thermal runaway. The reason

to why Fernandes found smaller ignition delay times could be that their mixtures contains many compounds that the other studies did not find. The amount of the compounds were small, but together they might have changed the ignition time. The other compounds can be sorted based on the amount of H_2, CO_2 and CO in the mixtures. The Golubkov NMC/LCO mixture contained less CO_2 in comparison to Golubkov LFP and NMC and had a faster ignition time than them. The Yuan NMC 1 and 2 mixtures have a relative small amount of H_2 compared to the other Yuan mixtures and that might be the reason why they have slower ignition times.

It is expected that the composition of the mixture would determine the ignition delay time, however it was not expected that mixtures from the same type of battery would not have similar ignition times. This could be some sort of artifact from the measurements of the vented gases as most teams doing those studies have used different methods and have been looking for different compounds.The gases vented from a thermal runaway have different compositions during the thermal runaway and cannot be excluded that some of the compounds could react even in the absence of an oxidizer. Some of the components, like DMC, contain some oxygen and it is not impossible that it could react even outside the battery. The difference between the studies could, in other words, be caused by the difference in measurement method. Another source of uncertainty could come from the batteries themselves. This report has divided the batteries into types mainly based on the composition of their cathode. This might be inadequate as the source of the gases lies in the electrolyte. As such, it might be more important to categories the batteries by their electrolyte and not their cathodes to fully compare the batteries used in different studies.

Comparing the original mechanisms with the new combined mechanism showed that the relative difference between the new and old is mostly less than 10%. This seems to be an acceptable margin of error for this project as the main point of the project is to find the general trends and not the specific values for any given mixture or equivalence ratio. However, it is worrying that a clear trend can be seen in figure 11 where the relative difference goes from negative to positive as the temperature decreases. Both mechanisms are not very old and have been made by competent people with up to date thermodynamic data. It would however have been better to use a mechanism that has been experimentally tested and verified. Another reason to why the trend exists for the relative differences of the CH_3F–HF mixtures could be that the F-mech contains a simpler hydrocarbon chemistry than the DMC-mech and DMC+F-mech. The hydrocarbon chemistry can also not be taken away from the fluorinated hydrocarbons as they become the same compounds as the hydrocarbons when the fluorine has been taken away, which will happen during the combustion process.

5.2 Flame speed

The equivalence ratio had a large effect on the flame speed of any given mixture. It was expected that the flame speed will decrease drastically as the equivalence ratio diverges from unity. If the equivalence ratio is to large or small then there will be a lot of fuel or oxygen that needs to be heated, but does not contribute to the combustion. It was also expected that the highest flame speeds were not reached at a equivalence ratio of 1, but at a slightly higher value. This is common in the field of combustion and the reason for this is that in a stoichiometric mixture, all fuel and oxygen will not react. In the beginning of the reaction, there is a lot of both, but as the combustion process progresses, the concentration of both decreases. At the end most of both have been used up, but not everything. To maximize the amount of energy one gets from the combustion, one should add more fuel to the mixture. This uses up all of the oxygen in the combustion. The fuel that has not fully reacted can still contribute to the energy output by a partial reaction. That is why the flame speed maximum is found at the equivalence ratio of 1.1 and not 1.0 for DMC. It should be noted that the maximum flame speed changes based on the mixture. The DMC–CO mixture has a maximum that moves from 1.1 to 1.5 when the mixture contains much CO. The reason for this is probably that CO needs much less oxygen than the other compounds used in this project and it is therefore required to add more CO than for example DMC to get the same effect.

The flame speed changes with the composition of the mixture. Pure DMC has a maximum flame speed of roughly 30 cm/s and pure C_2H_4 has a maximum of roughly 65 cm/s. All the mixture combinations of DMC

and C_2H_4 have flame speeds in between. Once again, the trend is not necessarily linear and varies between the mixtures. The DMC–C_2H_4 mixture on first inspection seems to have a linear relation between the flame speed and the mixture composition, but if one looks closely, one can see that the mixtures with much DMC are more similar to each other than the mixtures with much C_2H_4.

The ignition time for DMC and CO was very similar and one could not properly tell if the mixture followed the same trend as all the others. When it comes to the flame speeds, it is easy to tell them apart as they have completely different flame speeds. CO has a maximum flame speed that is twice that of DMC, and the maximum is also at a different equivalence ratio. It seems therefore likely that the DMC–CO mixtures follows both the ignition time and flame speed trends.

It is much clearer for the flame speed than for the ignition time that having complete combustion products in the mixture has a slowing effect on the combustion. The DMC–CO_2, Other 6 and CH_3F–HF mixtures show that the flame speed trends towards zero as the fraction of CO_2 or HF increases. However, it is strange that the DMC–HF mixtures show very little effect when the amount of HF is increased. It is a smaller increase than for the other mixtures, but the increase in HF is large enough that it was noticeable. The other fluorinated compound mixtures also show a very small effect from the fluorinated compounds. It should be noted that the only compound that decreased the flame speed of DMC was HF. This, together with the lack of change in the ignition time, indicates that the fluorinated compounds have a different chemistry than the hydrocarbons and that is the reason why no large effect of the mixing can be seen. An in–depth study of the reactions involved could give further answers, but there was not enough time to preform that in this project.

The flame speed of the different battery types were different. The flame speed from the Fernandes mixtures are closer to that of the Golubkov LCO/NMC mixture, which is strange as Fernandes measured on a LFP batttery. The Yuan LFP had higher flame speeds than in Fernandes study, and Golubkov LFP had much higher flame speeds than in the other two studies. The Golubkov NMC mixture had flame speeds that are in line with the flame speeds from the Yuan NMC 1 and 2 mixtures. The flame speed is much more sensitive to the composition of the mixture, than the ignition delay time and the difference in flame speed can to some extent be explained. However, this can not explain the trend seen in the Golubkov mixtures where LFP has the highest amount of CO_2 and LCO/NMC the lowest. One would expect the fastest flame speeds to come from the mixture with the lowest amount of CO_2. The flame speed seems to decrease as the amount of CO increases in the mixture. The other compounds have roughly the same concentration for all of Golubkov mixtures. The Yuan NMC 1 mixture contained less CO_2 and more CO than Yuan NMC 2, which could explain why it had higher flame speeds. The Yuan LFP mixture contains more H_2 than Yuan NMC 1 and NMC 2 and it is expected that it would have faster flame speeds, but it does not. The reason for this might be that Yuan LFP contains more CO_2. It should be noted that this is a rather simple analysis of the compounds of the mixtures and that the flame speeds are probably affected by the other compounds not mentioned in this analysis that are in the mixtures.

The mechanism comparison is similar to the one for the ignition time. The relative differences for the DMC–C_2H_4 mixtures is mostly random, while it has a clear trend for the CH_3F–HF mixtures. However, the relative differences are small and could have been caused by the numerical nature of the simulations.

6 Outlook

This project is a part of a larger project done in collaboration between Lunds university and Uppsala university. The research done in Uppsala will focus on detecting all of the compounds released after a thermal runaway using mass spectrometry. The research in Lunds university will then use that data to construct high precision optical experiments that can measure the concentration of some of the species as they are burning. This will then be used to create and validate chemical kinetic mechanisms for computer simulations of battery fires.

This project could be improved mainly in three different way. One could dive deeper into the simulations that have already been done and analyse the reactions of the simulations. This would explain which reactions are important and why some mixtures got higher or lower ignition times or flame speeds. Another direction a future project could take is to examine more species or how the properties of three-component gas mixtures changes as the composition of the mixtures changes. A third direction of future research is to develop the kinetic mechanism. The mechanisms were chosen because they could handle DMC or fluorinated compounds. One could make a mechanism that can handle larger carbonates or a mechanism with more advanced hydrocarbon chemistry as well as fluorinated compounds. However it should be mentioned that Linteris et al. are currently developing their kinetic mechanism.

7 Acknowledgments

Elna Heimdal Nilsson for guiding me through this project and Ulf Ryde for proofreading this rapport.

References

[1] European Automobile Manufactures Association. Accessed 23 April 2021. https://www.acea.be/statistics/tag/category/share-of-diesel-in-new-passenger-cars

[2] J. Braun, H. Stöß, A. Zober, *Intoxication following the inhalation of hydrogen fluoride*

[3] M. Lindkvist, *Electriska fordon och räddning: En inhämtning av erfarenheter från fältet och rekomenderade arbetssätt*, MSB 1533, April 2020, ISBN 978-91-7383-29-2

[4] R. Garcia-Valle, J.A.P. Lopes, *Electric vehicle integration into modern power networks*, Springer, New York, 2013

[5] *SAMSUNG SDI The composition of EV batteries: cells? Modules? Packs? Let's understand properly!* http://www.samsungsdi.com/column/all/detail/54344.html, Accessed on 9 May 2021

[6] A. Dinger et al., *Batteries for electric cars: challenges, opportunities, and the outlook to 2020*, The Boston Consulting Group, 2013

[7] P. Sun, R. Bisschop, H. Niu, *A Review of Battery Fires in Electric Vehicles*, Fire Technology, 56, 1361–1410, 2020, https://doi.org/10.1007/s10694-019-00944-3

[8] R. Von Burg, *Toxicoly update*, J. Appl. Toxicol. 19 (1999), p. 379–386,

[9] D. Sturk, L. Rosell, P. Blomqvist, A.A. Tidblad, *Analysis of Li-Ion Battery Gases Vented in an Inert Atmosphere Thermal Test Chamber*, Batteries 5 (2019) 61

[10] F. Larsson, P. Andersson, P. Blomqvist, B.E. Mellander, *Toxic fluoride gas emissions from lithium–ion battery fires*, Scientific reports 7 (2017) 10018, DOI:10.1038/s41598-017-09784-z

[11] Y. Fernandes, A. Bry, S. de Persis, *Identification and quatification of gases emitted during abuse tests by overcharge of a commercial Li-ion battery*, J. Power Sources 387 (2018) 106–119, https://doi.org/10.1016/j.jpowsour.2018.03.034

[12] A.W. Golubkov et al., *Thermal–runaway experiments on consumer Li-ion batteries with metal-oxide and olivin-type cathodes*, RSC Adv. 4 (2014) 3633, DOI: 10.1039/c3ra45748f

[13] L. Yuan et al., *Experimental study on thermal runaway and vented gases of lithium–ion cells*, Process. Saf. Environ. Prot. 144 (2020), p. 186–192, https://doi.org/10.1016/j.psep.2020.07.028

[14] F. Larsson et al., *Gas explosions and thermal runaways during external heating abuse of commercial lithium–ion graphite–$LiCoO_2$ cells at different levels of ageing*, J. Power Sources 373 (2018), p. 220–231, https://doi.org/10.1016/j.jpowsour.2017.10.085

[15] B. Truchot, F. Fouillen, S. Collet, *An experimental evaluation of toxic gas emissions from vehicle fires*, Fire Safety J. 97 (2018), p. 111–118, https://doi.org/10.1016/j.firesaf.2017.12.002

[16] A. Lecocq et al., *Scenario–based prediction of Li-ion batteries fire-induced toxicity*, J. Power Sources 316 (2016), p. 197–206, http://dx.doi.org/10.1016/j.jpowsour.2016.02.090

[17] Hilbert R., Tap F., El-Rabii H., Thévenin D., *Impact of detailed chemistry and transport models on turbulent combustion simulations*, Prog energy combust sci, 2004; 31:61–117

[18] D.R. Burgess, M.R. Zachariah, W. Tsang, P.R. Westmoreland, *Thermochemical and chemical kinetic data for fluorinated hydrocarbons*, Prog. Energy Combust. Sci. 21 (1996), p. 453–529, https://doi.org/10.1016/0360-1285(95)00009-7

[19] Curran H.J, Gaffuri P, Pitz W.J, Westbrook C.K., *A comprehensive modeling study of n-heptane oxidation*, Combust Flame 1998;114:149–77

[20] Turányi T., Tomlin A.S., *Analysis of Kinetic Reaction Mechanisms*, Berlin: Springer; 2014. p. 6-28

[21] Seinfeld J.H., Pandis S.N., *Atmospheric Chemistry and Physics: From Air Pollution to Climate Change*, Second edition, John Wiley and Sons, 2006, Chapter 3.5

[22] Atkins P., de Paula J., *Physical chemistry*, 10th edn., Oxford, Oxford university press, 2014, p. 837-848

[23] K. Alexandrino, M.U. Alzueta, H.J. Curran, *An experimental and modeling study of the ignition of dimethyl carbonate in shock tubes and rapid compression machine*, Combust. Flame 188 (2018), p. 212–226, https://doi.org/10.1016/j.combustflame.2017.10.001

[24] G. Linteris, V. Babushok, *Laminar burning velocity predictions for C_1 and C_2 hydrofluorocarbon refrigerants with air*, J. Fluorine chem. 230 (2020) 109324, https://doi.org/10.1016/j.jfluchem.2019.05.002

[25] G.P. Smith et al., GRI Mech 3.0, (2015) Sept. 9 http://www.me.berkeley.edu/gri_mech.

[26] CHEMKIN-PRO 15142; Reaction Design: San Diego, CA, 2015.

8 Appendix

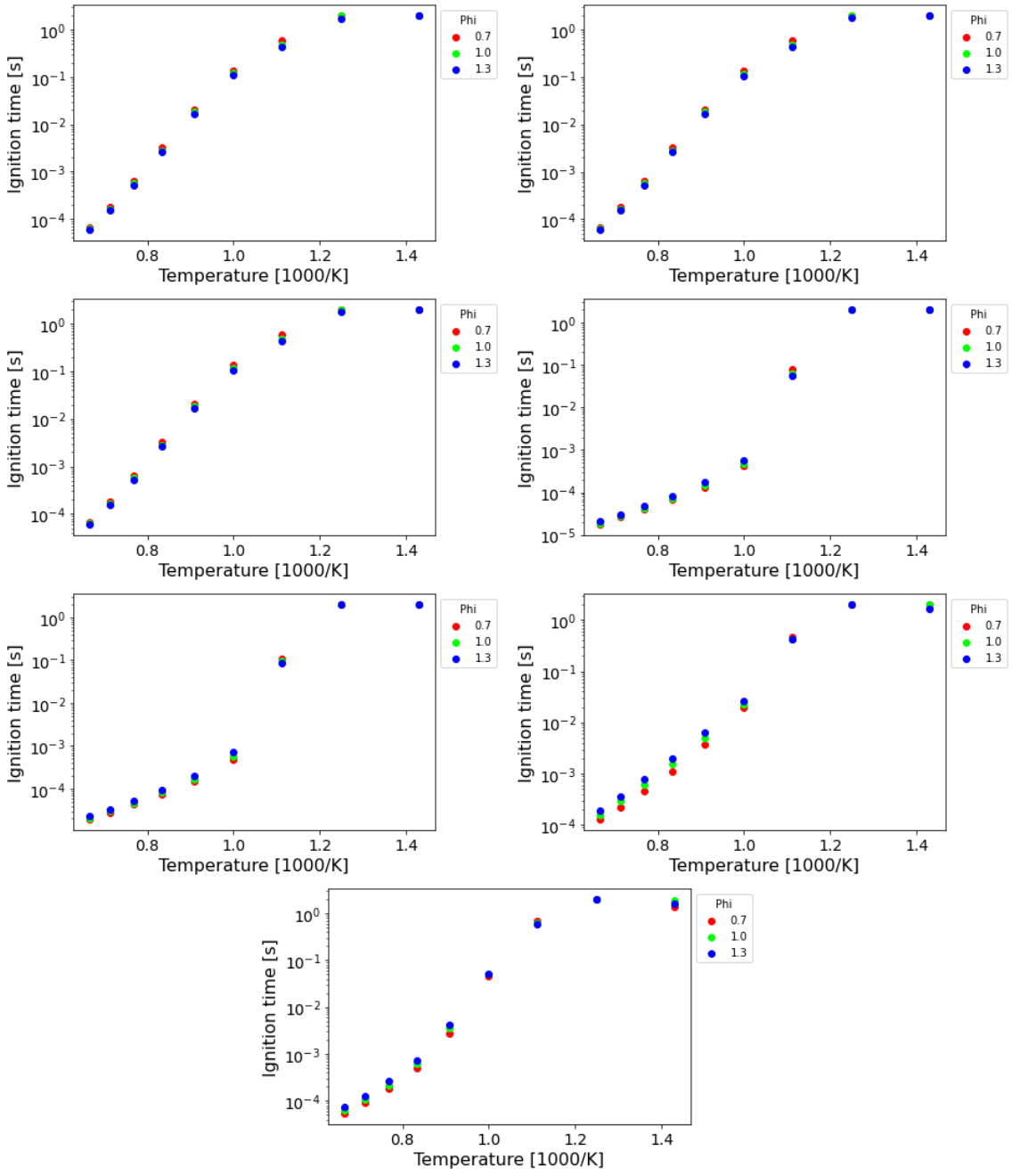

Figure 20: Ignition time for the Others 1-5, 8 and 9.

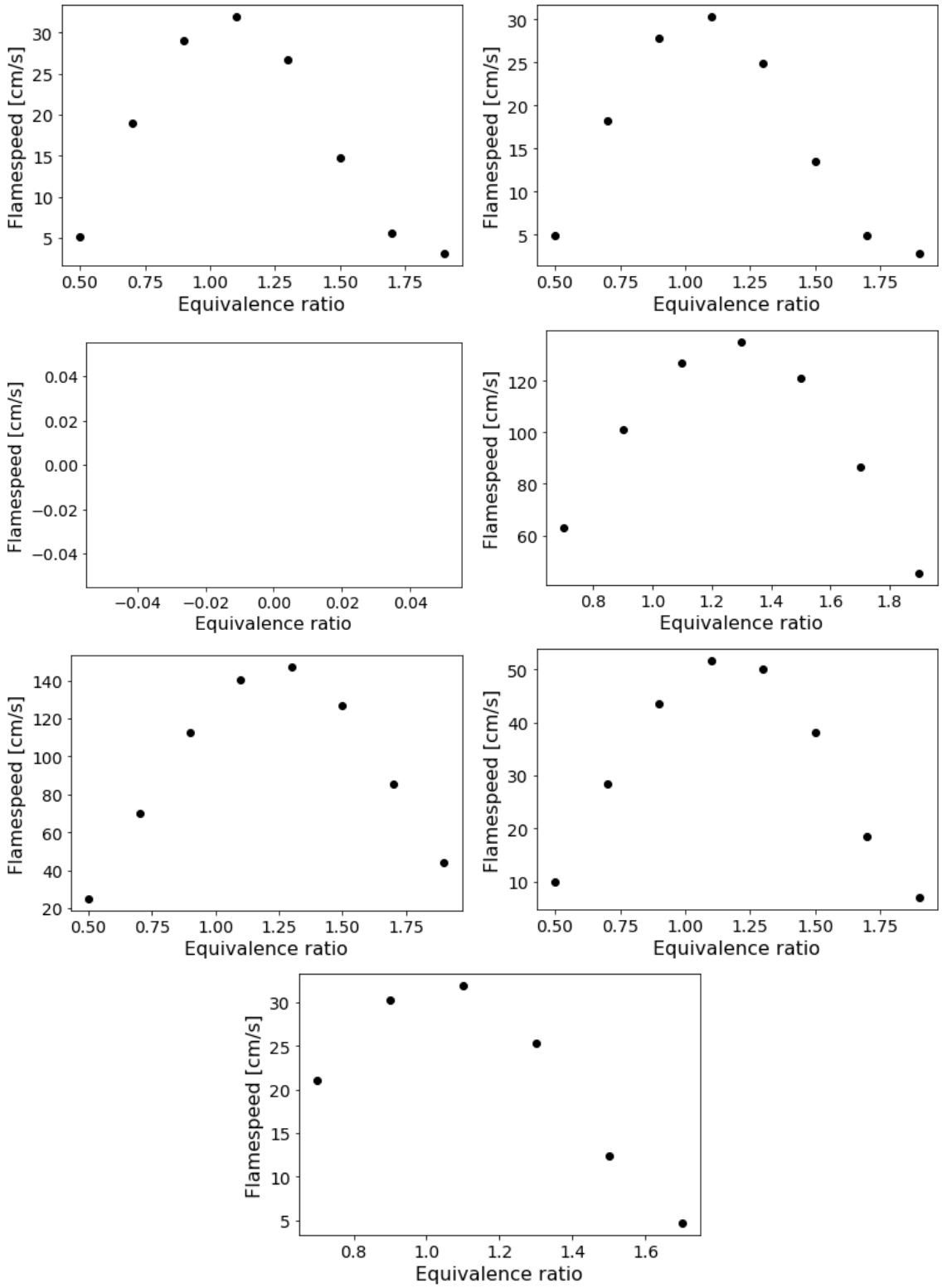

Figure 21: Flame speed for the Others 1-5, 8 and 9.